JOURNAL OF BACTERIOLOGY, Nov. 2011, p. 5914–5922 Vol. 193, No. 21
0021-9193/11/$12.00 doi:10.1128/JB.05458-11

Adjusting the Spokes of the Flagellar Motor with the DNA-Binding Protein H-NS▽†

Koushik Paul, William C. Carlquist, and David F. Blair*

Department of Biology, University of Utah, Salt Lake City, Utah 84112

Received 3 June 2011/Accepted 22 August 2011

The H-NS protein of bacteria is a global regulator that stimulates transcription of flagellar genes and that also acts directly to modulate flagellar motor function. H-NS is known to bind FliG, a protein of the rotor that interacts with the stator and is directly involved in rotation of the motor. Here, we find that H-NS, well known for its ability to organize DNA, acts in the flagellar motor to organize protein subunits in the rotor. It binds to a middle domain of FliG that bridges the core parts of the rotor and parts nearer the edge that interact with the stator. In the absence of H-NS the organization of FliG subunits is disrupted, whereas overexpression of H-NS enhances FliG organization as monitored by targeted disulfide cross-linking, alters the disposition of a helix joining the middle and C-terminal domains of FliG, and enhances motor performance under conditions requiring a strengthened rotor-stator interface. The H-NS homolog StpA was also shown to bind FliG and to act similarly, though less effectively, in organizing FliG. The motility-enhancing effects of H-NS contrast with those of the recently characterized motility inhibitor YcgR. The present findings provide an integrated, structurally grounded framework for understanding the roughly opposing effects of these motility regulators.

Many species of bacteria swim using rotating flagella powered by the membrane ion gradient (3, 19, 21, 30). In *Escherichia coli*, assembly and operation of the bacterial flagellum depends on the products of more than 50 genes, expressed from operons organized in a three-tier regulatory hierarchy with the master regulatory *flhDC* genes at the top (3, 14, 37). A complex of the FlhD and FlhC proteins directs transcription of genes in the second regulatory class, which encode components of the flagellar basal structure. Genes in the third class encode late-assembled proteins including the flagellin subunits forming the flagellar filament, the MotA and MotB proteins that energize rotation, and components of the chemosensory pathway. The DNA-binding protein H-NS is needed for normal expression of *flhDC*, and cells deleted for *hns* are unable to assemble flagella (5, 26, 53). H-NS has also been shown to be important for optimal function of the assembled flagellum (26), but its specific role in enabling motor rotation has not been determined.

The nonrotating part of the flagellar motor, or stator, is formed from the membrane proteins MotA and MotB, present in complexes with the composition $MotA_4MotB_2$ (29, 50). Each motor contains several (11 or more) stator complexes, which surround the rotor and function independently to generate torque (7, 9, 25, 29, 46, 50). The stator complexes conduct the energizing protons (or Na^+ ions in the motors of some alkalophilic or marine species) and harness ion flow to rotation by a mechanism that appears to involve conformational changes in the stator induced by proton binding to a critical Asp residue of MotB (4, 6, 28, 70). The key part of the rotor is formed from the proteins FliG, FliM, and FliN. These form a large assembly called the switch complex that is essential for rotation and that controls the reversals in motor direction that are the basis of chemotaxis (18, 22, 35, 52, 65, 67).

FliG is the rotor protein involved most closely in torque generation (22, 35). Portions of the FliG C-terminal domain ($FliG_C$) are dispensable for flagellar assembly but essential for motor rotation, and experiments in a variety of species have shown that conserved charged residues in this domain interact with conserved charged residues of the stator protein MotA (34, 64, 68, 69). We recently proposed a structural model for the switch complex, which was developed on the basis of crystal structures of the components together with binding, cross-linking, and mutational experiments to probe their arrangement (11, 12, 31, 40–42, 44, 49) (Fig. 1). FliG is positioned at the top (the membrane-proximal part) of the switch complex to allow interaction with the stator, and the middle domain of FliM ($FliM_M$) is situated below FliG (Fig. 1). Several studies have indicated that the motor contains more copies of FliM than FliG (about 34 and 26 subunits, respectively) (17, 54, 58, 59, 66), and FliM has been shown to interact with at least two distinct sites on FliG, a conserved hydrophobic patch on $FliG_C$ and a conserved EHPQR motif on the middle domain ($FliG_M$) (13, 43). In our working model of the switch complex, both observations are accounted for by hypothesizing two distinct arrangements for $FliM_M$; most $FliM_M$ domains are positioned under $FliG_C$, where they interact with the hydrophobic patch and form the outer part of the C ring, whereas a subset of about eight $FliM_M$ domains are tipped inward to interact with $FliG_M$ (13, 43) (Fig. 1). The lower part of the C ring is formed by FliN and the C-terminal domain of FliM ($FliM_C$) (49). FliM and FliN function together in receiving signals from the chemotaxis signaling pathway: the clockwise-signaling molecule phospho-CheY is captured by a segment near the N terminus of FliM (61) and subsequently interacts with a site on FliN to induce relative subunit movements in the lower part of the C ring (48, 49). These movements must be transmitted "up"

* Corresponding author. Mailing address: Department of Biology, University of Utah, Salt Lake City, UT 84112. Phone: (801) 585-3709. Fax: (801) 581-4668. E-mail: blair@bioscience.utah.edu.

† Supplemental material for this article may be found at http://jb.asm.org/.

▽ Published ahead of print on 2 September 2011.

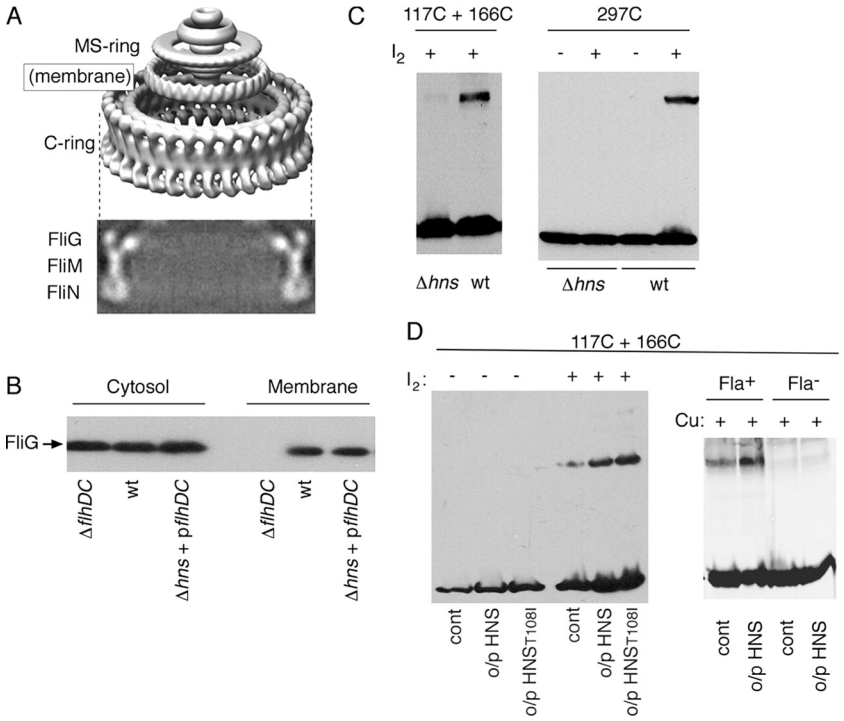

FIG. 1. Role of H-NS in the organization of FliG. (A) EM reconstructions of the basal body of *Salmonella* (reprinted from reference 58 with permission). The lower view shows a cross section through the C ring with the approximate positions of the switch complex proteins indicated. (B) Membrane localization of FliG in a Δ*hns* mutant. FliG was expressed from a plasmid in cells deleted for the master regulator genes *flhDC* (Δ*flhDC*), in wild-type cells, or in cells deleted for *hns* and expressing the flagellar master regulatory genes from a plasmid (Δ*hns* + p*flhDC*). Following separation into membrane and soluble fractions, proteins were resolved by SDS-PAGE and detected by immunoblotting with anti-FliG antibody. (C) Effects of H-NS deletion on FliG organization, probed by targeted FliG-FliG disulfide cross-linking in intact cells. Plasmids expressing the FliG mutants with Cys replacement residues at positions 117 and 166 (177C + 166C) or at 297 (297C) were introduced into the Δ*fliG* or Δ*fliG* Δ*hns* strain. Cross-linking was induced using iodine (0.2 mM), and products were characterized on immunoblots using anti-HA antibody. (D) The left panel shows increased cross-linking through the FliG middle domain in intact cells overexpressing wild-type H-NS or the H-NS variant T108I that exhibits enhanced FliG binding. Cross-linking was induced with iodine, and the blot was probed with anti-HA antibody. The right panel shows a comparison of cross-linking through the FliG middle domain in the Δ*fliG* background (which assembles flagella when the Cys-containing FliG protein is expressed from a plasmid) and in a nonflagellate Δ*flhDC* strain, with H-NS present either at normal levels (cont) or overexpressed (o/p). Cross-linking was induced with Cu-phenanthroline, and the blot was probed with anti-HA antibody.

through the other parts of the C ring to trigger changes at the rotor-stator interface, but the switching movements in the upper part of the ring have not yet been defined.

Besides its interactions with other flagellar proteins, FliG also interacts with the cyclic-di-GMP (c-di-GMP) binding protein YcgR (16, 45) and the small nucleoid-structuring protein H-NS (15, 38). In response to increased levels of c-di-GMP, YcgR downregulates flagellar motility by mechanisms that have been characterized in some detail (10, 16, 45). The action of H-NS at the motor has not been explored as closely. H-NS is a global regulator that binds diverse regions of the chromosome and acts in most cases to repress transcription (47). One of the genes repressed by H-NS is *hdfR*, which encodes a repressor of *flhDC*; thus, H-NS acts to stimulate flagellar gene expression, and Δ*hns* mutants of *E. coli* are nonflagellate (5, 26, 53). Ko and Park found that when a Δ*hns* strain was engineered to express *flhDC* constitutively (Δ*hns flhDC*-constitutive strain) the cells assembled flagella but were still only poorly motile, indicating a role for H-NS in motor rotation (26). Marykwas et al. (38) and Donato and Kawula (15) showed that H-NS interacts with FliG and proposed that this interaction might modulate the function of the motor. In a recent study employing fluorescent resonance energy transfer (FRET) methods, the interaction of H-NS with FliG was confirmed, and an additional interaction involving FliN was suggested (32).

Details of H-NS binding to FliG and the mechanism by which it enhances motor rotation are unknown. Here, we examine the molecular details and functional consequences of the H-NS/FliG interaction. The results indicate that H-NS, well known for its ability to organize DNA, acts in this setting to organize the upper part of the rotor, in essence tightening the spokes. H-NS binds to the EHPQR motif in $FliG_M$, affecting structural elements that are in a bridging position between the inner parts of the rotor and the outer (i.e., closer to the edge) parts that interact with the stator to enable rotation. Motors operating with the assistance of H-NS can function better under conditions of high ionic strength or high load or in the presence of mutations that weaken the rotor-stator interface. The H-NS homolog StpA was found to act similarly and to partially substitute for H-NS function in a Δ*hns* strain. The possible significance of an H-NS-based mechanism for motor regulation is discussed.

MATERIALS AND METHODS

Strains and media. The *E. coli* strains and plasmids used are listed in Table S1 in the supplemental material. Procedures for transformation and plasmid isolation were as described previously (55, 56). TB medium contained 10 g of tryptone and 5 g of NaCl per liter. Ampicillin was used at 125 μg/ml in liquid medium or at 50 μg/ml in soft-agar motility plates. Chloramphenicol was used at 50 μg/ml in liquid medium and at 12.5 μg/ml in motility plates. Isopropyl-β-D-thiogalactopyranoside (IPTG) and sodium salicylate were prepared as 0.1 M and 10 mM aqueous stocks, respectively.

Mutagenesis, cross-linking, and binding assays. Site-directed mutagenesis was carried out on the *hns* (pKP58 and pKP74) or *stpA* (pKP181) templates according to the Quick Change protocol (Stratagene, La Jolla, CA). Mutations were confirmed by sequencing.

Targeted disulfide cross-linking experiments were carried out essentially as described by Lowder et al. (36). Cross-linking was induced using iodine or Cu-phenanthroline, as described previously (36, 42). Cross-linking used intact cells or cells lysed using lysozyme/EDTA/osmotic shock, as indicated in the figures. Products of cross-linking were examined on immunoblots using anti-FliG or anti-hemagglutinin (HA) antibody, as indicated on the figures. Epitope-tagged FliG had the HA antigen fused to the C terminus of the protein through a linker of five alanine residues.

Binding of FliG to H-NS and StpA was measured using a glutathione *S*-transferase (GST) pulldown assay. Proteins were expressed separately in two strains, using plasmid pHT100 (57) derivatives to express the GST fusions to H-NS or StpA (and their mutant variants) and using pSL27 (69) to express FliG (or its variants). Control experiments used GST only, expressed from plasmid pHT100. The parent strain was RP3098 (Δ*flhDC*), which expresses no flagellar genes from the chromosome. Cells were cultured overnight at 32°C in 40 ml of TB medium containing appropriate antibiotics and 400 μM IPTG. Cells were harvested and resuspended in lysozyme-containing buffer as described previously (39). After 1 h on ice, cells were disrupted by sonication. Debris was pelleted (16,000 × *g* for 40 min at 4°C), and 50 μl of the supernatant was saved for use in estimating the amount of FliG present before addition of affinity beads. The rest (~1 ml) was transferred to a clean tube, mixed with 150 μl of a 50% slurry of glutathione-Sepharose 4B (Pharmacia) prepared according to the manufacturer's directions, and incubated for 1 h at room temperature with gentle rotation to allow binding. The Sepharose beads were then pelleted by a 1-min microcentrifuge spin, washed twice with 1 ml of phosphate-buffered saline containing 1% bovine serum albumin (BSA) and 0.1% Triton-X, and pelleted again by a brief spin. The beads were then incubated with 50 μl of elution buffer (50 mM reduced glutathione in 50 mM Tris-HCl [pH 8]) for 10 min at room temperature with gentle rotation to release the GST–H-NS/GST-StpA and associated proteins. Beads were then pelleted, and the supernatant was collected for analysis by SDS-PAGE and immunoblotting using anti-FliG antibody (57).

Membrane isolation. MS296 (wild type [wt]), MS1162 (Δ*hns*), and RP3098 (Δ*flhDC*) strains expressing p*flhDC* from a plasmid (pKP85) were transformed with plasmid pSL27 (69) expressing FliG. Cells were cultured overnight at 37°C in 10 ml of LB medium with appropriate antibiotics. Cell density was measured, and cells were pelleted and resuspended in lysis buffer (50 mM Tris, pH 8.0, 500 mM NaCl, 1 mM EDTA, 0.2 mg/ml lysozyme) using a volume (minimally 1 ml) adjusted to give constant cell density. Cells were incubated on ice for 1 h, sonicated for 1 min, and centrifuged (16,000 × *g* at 4°C for 30 min) to separate membrane and cytosolic fractions. Pellets (the membrane fraction) were resuspended in gel-loading buffer containing SDS and 2-mercaptoethanol. The supernatant (cytosolic fraction) was transferred to a fresh tube, mixed with 110 μl of trichloroacetic acid solution, placed on ice for 10 min, and then centrifuged (16,000 × *g* at 4°C for 10 min). Precipitated protein was resuspended in gel-loading buffer. Samples of the cytosolic and membrane fractions were electrophoresed on SDS-PAGE gels and immunoblotted with anti-FliG antiserum.

Assays of motility. Motility in soft agar was measured essentially as described by Tang et al. (56), using deletion strains (see Table S1 in the supplemental material) transformed with plasmids encoding the corresponding wild-type or mutant proteins. Soft-agar plates contained 0.27% agar, antibiotics, and inducers (IPTG or Na-salicylate) at the concentrations indicated in the figures or figure legends. To examine effects of overexpressed StpA (pKP181) and StpA with the mutation F21C [StpA(F21C)] (pKP211) in the *hns* null strain, cells of strain MS1162 (Δ*hns*) containing the *flhDC* expression plasmid (pKP85) were transformed with the relevant plasmids, and expression was induced using 2.5 μM Na-salicylate. Controls were transformed with the parent vectors pKG116 and pTBM30. Assays of surface swarming used LB plates containing 0.5% glucose and 0.5% Eiken agar.

SDS-PAGE and immunoblotting. Protein samples were separated on 10% SDS-PAGE minigels (Bio-Rad MiniProtean system) and transferred to nitrocellulose using a semidry transfer apparatus (Bio-Rad). Rabbit polyclonal antibody against FliG was prepared as described previously (35) and used at a 1,500-fold dilution. FliG HA-tagged proteins were detected by mouse anti-HA antibody using a 1:1,000-fold dilution (Covance). Bands were visualized using the Super Signal West Picoluminol system (Pierce) and quantified by video densitometry using NIH ImageJ (http://rsbweb.nih.gov/ij).

RESULTS

H-NS is not required for localization of FliG to the motor. Because H-NS is required for normal flagellar rotation (26) and interacts with the torque-generating component FliG (15, 38), we first examined the membrane localization of FliG in cells lacking H-NS. Cells deleted for *hns* but constitutively expressing *flhDC* were cultured and separated into membrane and soluble fractions, and immunoblots were used to estimate FliG levels in the fractions. A positive control used wild-type cells, and the negative control used the Δ*flhDC* strain, which expresses no flagellar genes from the chromosome. Plasmid-expressed FliG protein was found in only the soluble fraction in Δ*flhDC* cells, indicating that localization to the membrane does not occur in the absence of flagella. In wild-type cells, about half of the FliG was observed in the membrane fraction, presumably reflecting its association with flagellar structures. The level of membrane-associated FliG was the same in the Δ*hns* strain as in the wild type (Fig. 1B). Thus, localization of FliG to the membrane requires the presence of flagella but does not require H-NS.

H-NS affects the organization of FliG. Because FliG is closely involved in motor rotation, the proper organization of FliG subunits in the rotor is expected to be important for motility. The arrangement of FliG subunits in the rotor was examined previously using targeted disulfide cross-linking, and Cys replacements enabling high-yield disulfide formation were identified in both the middle and C-terminal domains (36). To determine whether FliG organization is altered in the absence of H-NS, we tested cross-linking of these Cys-substituted FliG proteins in the Δ*hns* background. Disulfide bond formation was induced using iodine, and cross-linked products were examined on immunoblots. Detection was facilitated by attachment of an HA tag to the C terminus of FliG, which allowed the protein to function in both flagellar assembly and motility, as assayed by complementation of a Δ*fliG* strain (see Fig. S1 in the supplemental material). FliG-FliG cross-linking was similar to that reported previously in the wild-type background, but in cells lacking H-NS, FliG cross-linking through both the middle and C-terminal domains was greatly diminished (Fig. 1C). Conversely, when H-NS was overexpressed in cells, cross-linking through the middle domain was enhanced (Fig. 1D). The FliG-FliG cross-linking induced by H-NS appears to occur within assembled motors because it was not observed when the experiment was carried out in a Δ*flhDC* strain that does not assemble flagella (Fig. 1D). We conclude that H-NS influences the organization of FliG subunits in the motor.

Mapping the FliG–H-NS interaction. Previous genetic (38) and biochemical (15) studies gave evidence that H-NS interacts with FliG. To examine this interaction further, we measured binding of H-NS to FliG using a pulldown assay with a

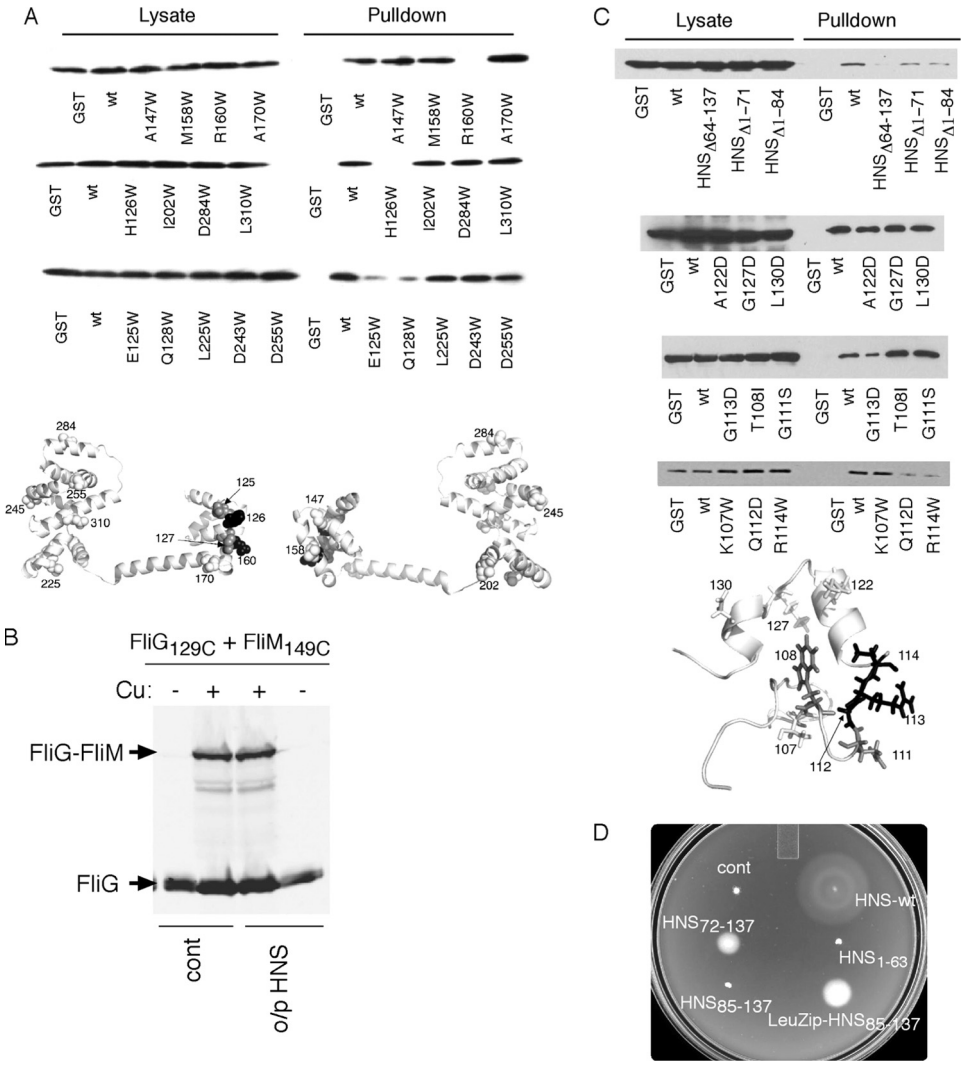

FIG. 2. Mapping the FliG-H-NS interaction. (A) Coisolation of FliG with GST–H-NS and effects of FliG mutations on the binding. FliG was detected using anti-FliG antibody. In the lower part of the panel, the effects of the mutations are mapped onto the structure: black, binding eliminated; gray, binding weakened; white, binding similar to that of the wild type. (B) Cross-linking between Cys residues at positions 149 of $FliM_M$ and 129 of $FliG_M$ at normal levels of H-NS(cont, constitutive) and with H-NS overexpressed (o/p). The blot was probed with anti-HA antibody. This cross-link is diagnostic of the inward-tipped $FliM_M$ domains that interact with the EHPQR motif of $FliG_M$ (43). FliG-FliM cross-linking was not affected by overexpression of H-NS. (C) Effects of H-NS deletions and point mutations on the binding to FliG. Effects are mapped onto the structure of the C-terminal domain of H-NS (Protein Data Bank [PDB] code 1hns) in the lower part of the panel: black, binding eliminated; dark gray, enhanced interaction with FliG; white, binding not affected. (D) Function of truncated H-NS variants. H-NS proteins were expressed in the Δ*hns flhDC*-constitutive strain from a salicylate-inducible plasmid (salicylate concentration, 2.5 μM). Fresh transformants were picked onto plates containing tryptone and 0.28% agar and incubated for 9 h at 32°C. LeuZip, leucine zipper.

GST–H-NS fusion. Wild-type FliG was reproducibly coisolated with GST–H-NS in this assay (Fig. 2). FliG proteins with Trp replacements in various surface positions (made for a previous study [13]) were used to map the site of H-NS interaction. Binding to H-NS was prevented by the replacements of residues His126 or Arg160 and was substantially weakened by replacements of Glu125 or Gln128 (Fig. 2A). These four residues comprise most of the EHPQR motif, a well-conserved surface feature of $FliG_M$ that has been shown to interact with FliM (13, 43). Several other positions on FliG were tested but did not affect the interaction with H-NS (Fig. 2). We conclude that the EHPQR motif on $FliG_M$ forms the binding site for H-NS. Note that binding of this motif to both H-NS and $FliM_M$ is permissible in the present model for the switch complex because most $FliM_M$ domains do not occupy the EHPQR motif but are in the outward position under $FliG_C$. To determine whether H-NS affects the distribution of $FliM_M$ domains between the inward and outward locations, we examined disulfide cross-linking between $FliM_M$ and $FliG_M$ through a previously identified Cys pair (position 149 of FliM and position 129 of FliG [$FliM_{149}$/$FliG_{129}$]). This cross-link was shown previously to form in moderate yield and is diagnostic of the inwardly positioned $FliM_M$ domains that contact the EHPQR motif of $FliG_M$ (43). The yield of this disulfide cross-link was not measurably affected by overexpression of H-NS (Fig. 2), indicating that excess H-NS does not drive additional $FliM_M$

TABLE 1. Motility of H-NS mutants

Mutation	Migration rate[a]
K107A	1.35
K107W	1.35
T108I	3.2
G111S	1.15
Q112D	0.35
G113D	0.3
R114A	1.0
R114W	0.35
A122D	0.75
G127D	0.9
L130D	2.35

[a] Rates of cell migration relative to wild-type controls measured in the same experiment. Data are for induction with 2.5 μM salicylate, which was optimal for all the mutants.

domains into the outward location and can bind readily enough to the EHPQR sites already available.

To examine determinants on the H-NS side of the interaction, the pulldown assay was employed with a collection of H-NS point mutants and deletion variants. FliG bound to all H-NS constructs that retained the C-terminal domain (data are shown for residues 72 to 137 of H-NS [H-$NS_{72–137}$] and H-$NS_{85–137}$; similar results were obtained for H-$NS_{52–137}$ and H-$NS_{62–137}$). The N-terminal domain of H-NS (residues 1 to 64) showed little, if any, interaction with FliG (Fig. 2B). Point mutations were in surface-exposed residues of H-NS and included a replacement (T108I) that was shown previously to strengthen the interaction with FliG (15), as well as the G111S and G113D mutations that were shown to weaken the binding to DNA (60). Mutant variants of H-NS were fused to GST, and pulldown experiments were performed as before. Binding to FliG was weakened by the H-NS mutations Q112D, G113D, and R114W, strengthened by the mutations T108I and G111S, and unaffected by the mutations K107W, A122D, G127D, and L130D (Fig. 2B). Residues 112 to 114 are grouped together in the C-terminal domain of H-NS, partially overlapping a surface implicated in binding to DNA (51, 60). To examine the functional consequences of the H-NS mutations, plasmids expressing the mutant H-NS variants were transformed into the Δ*hns* strain, and rates of migration in soft agar were measured (Table 1). Motility was reduced to about one-third of normal in the H-NS mutants with defects in FliG binding and was either unaffected or increased by the other H-NS mutations. Together, the binding and motility data indicate that the region around residues 112 to 114 of H-NS forms a functionally important contact with FliG.

Dimerization of H-NS is required for motility. H-NS is known to form stable dimers and higher oligomers (47). A study of deletion constructs showed that the self-association involves segments comprising residues 1 to 46 and residues 60 to 89 (8, 51). To examine the importance of H-NS oligomerization for flagellar motor function, we tested the function of H-NS proteins lacking these segments in a complementation assay using the Δ*hns* strain constitutively expressing *flhDC* (Δ*hns flhDC*-constitutive strain). As expected from the binding results, an H-NS protein lacking the C-terminal domain (H-$NS_{1–63}$) did not support motility. A construct lacking 71 N-terminal residues conferred weak motility, whereas one with an 84-residue deletion, and thus lacking almost all of the oligomerization determinants, was nonfunctional. When this H-$NS_{85–137}$ construct was fused to a leucine-zipper domain to induce dimerization, substantial motility was restored (Fig. 2C). Together, the results indicate that H-NS must form dimers to act effectively at the motor.

Similar action of the H-NS homolog StpA. Although the motility of the Δ*hns flhDC*-constitutive strain is poor, a small fraction of cells is observed to swim in liquid medium, and the strain retains some slight ability to migrate in soft agar (26). The *E. coli* chromosome encodes a protein called StpA that is related to H-NS, which retains both the dimerization domains and the residues implicated in FliG binding. To determine whether the residual motility in the Δ*hns* strain is due to StpA, we examined motility of a Δ*hns* Δ*stpA* strain. Motility of the double-deletion strain was no worse than that of the Δ*hns* parent. A Δ*stpA* strain (wild type for H-NS) exhibited nearly normal motility in soft agar, indicating that H-NS is more important than StpA for flagellar motor function (Fig. 3A). When provided at a high enough level, StpA appears able to substitute for H-NS: plasmid-expressed StpA restored motility

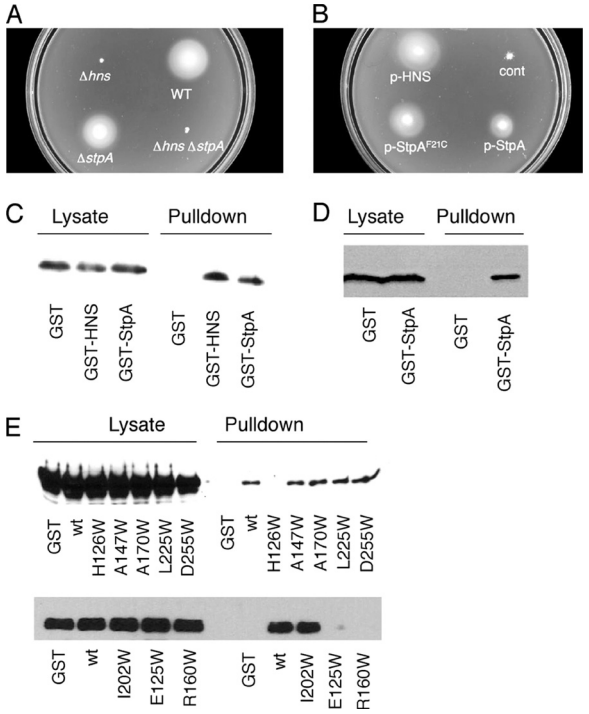

FIG. 3. Properties of the H-NS homolog StpA. (A) Soft-agar motility of Δ*hns*, Δ*stpA*, and Δ*hns* Δ*stpA* strains. Plates were incubated at 32°C for 10 h (salicylate concentration, 2.5 μM). (B) Partial complementation of a Δ*hns* mutant by overexpression of StpA and nearly full complementation by the more stable F21C variant. Cells contained the H-NS deletion and expressed *flhDC* constitutively. Plates were incubated at 32°C for 10 h. (C) Coisolation of FliG protein with GST–H-NS and GST-StpA. FliG was detected on immunoblots using anti-FliG antibody. This experiment used the *flhDC* null strain (RP3098), which expresses no chromosomal flagellar genes but retains the *hns* gene. (D) Coisolation of FliG with GST-StpA in a strain (MS299) that lacks H-NS. (E) Effects of mutations in FliG on its binding to StpA, measured in pulldown assays using a GST-StpA fusion. Blots were probed with anti-FliG antibody.

of the Δ*hns* cells to about half that observed on complementation with H-NS, and performance was improved further by use of the proteolysis-resistant variant StpA(F21C) (relevant because StpA is known to be relatively unstable in the absence of H-NS) (23, 24) (Fig. 3B).

Given this functional interchangeability, it seemed likely that StpA might also bind FliG. This was confirmed in a pulldown experiment using GST-StpA (Fig. 3C). StpA has been shown to form a heterodimer with H-NS (23), and so to rule out the involvement of an StpA/H-NS heterodimer, the pulldown experiment was also carried out in Δ*hns* cells. FliG was again coisolated with GST-StpA (Fig. 3D). To identify the binding regions on FliG, the experiment was carried out using the collection of FliG surface residue mutations. StpA binding was unaffected by mutations in FliG residues 147, 170, 202, 225, and 255 but was prevented by mutations in residues 125, 126, and 160, indicating a binding to the EHPQR motif similar to that of H-NS (Fig. 3E).

Overexpression of H-NS enhances motility in some circumstances. Given the importance of H-NS for FliG subunit organization, we were prompted to ask whether overexpression of H-NS might be beneficial for motor performance under any circumstances. Interactions at the rotor-stator interface appear to be largely electrostatic (64, 69), and motility in soft-agar plates is reduced under conditions of high ionic strength (27, 69). When H-NS was overexpressed, motility in standard soft-agar plates was not significantly affected, but the defect at high ionic strength (0.2 M to 0.3 M NaCl) was alleviated significantly (Fig. 4A). Further, a FliG mutant in which two of the interfacial residues are neutralized (D288N and D289N) exhibits a severe motility impairment that could be partially rescued by overexpression of H-NS (Fig. 4B). Because a stable rotor-stator interface might be especially important for cells migrating in relatively firm agar, we next examined H-NS effects on motility in plates containing more than the usual amount of agar (up to 0.42%). H-NS overexpression had little effect on motility in standard (0.27%) soft-agar plates but was clearly beneficial as agar concentration was increased to 0.39% or higher (Fig. 4C). At even higher agar concentrations, motility changed to a surface-associated swarming mode (20). H-NS proved especially important for swarming motility: cells expressing H-NS at a level sufficient to give strong motility in conventional motility plates were unable to swarm on 0.5% agar plates (Fig. 4D). Since H-NS is a positive regulator of *flhDC*, the improved motility at high salt and agar concentrations might be due to upregulation of all flagellar genes. To test this we compared the swarming of wild-type cells and cells overexpressing *flhDC* from an inducible plasmid. Overexpression of *flhDC* did not improve motility at either high salt or high agar concentrations (data not shown).

Further evidence of H-NS acting at $FliG_M$. The H-NS-binding site on $FliG_M$ lies near the helix that links this domain to $FliG_C$. The precise disposition of this helix is still uncertain as it occurs in different conformations in different crystal structures (11, 31, 40), but in any case it is expected to play an important role in the positioning of $FliG_C$. To probe the conformation of the linking helix and to look for the effects of H-NS, we introduced Cys residues in positions that are in proximity in a recent crystal structure (31) and measured yields of intramolecular cross-linking. Two Cys pairs were made.

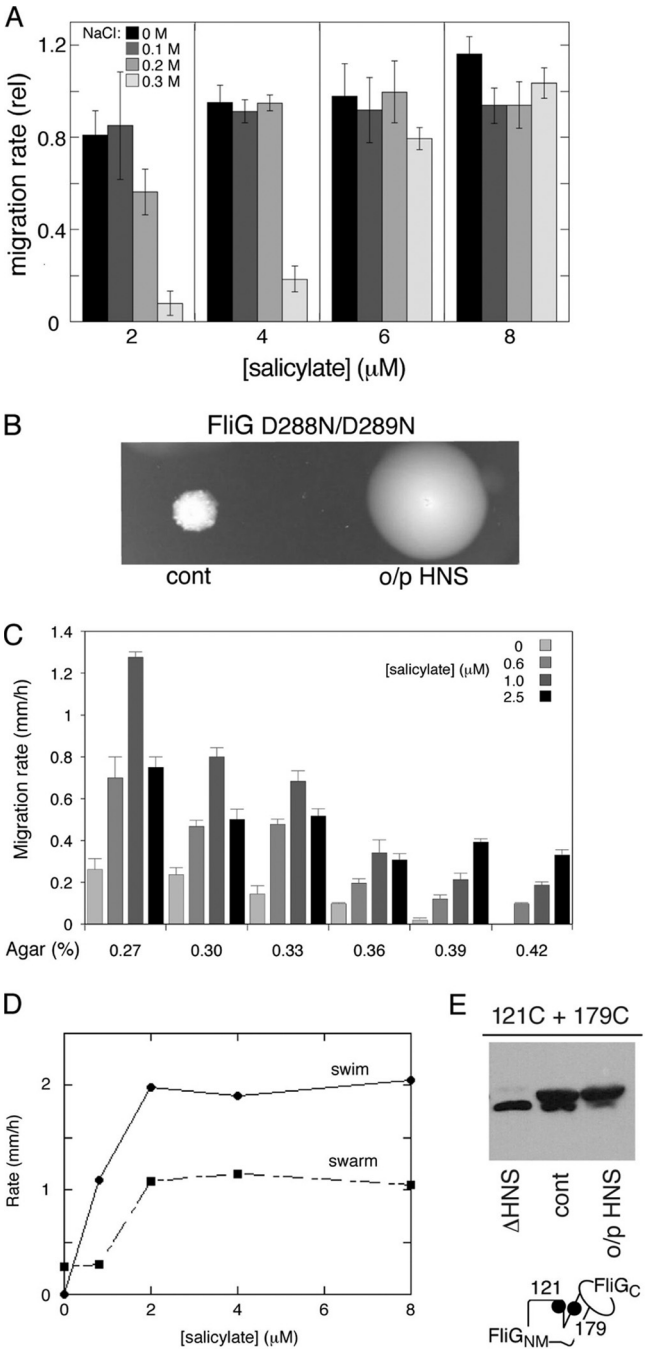

FIG. 4. Effects of H-NS overexpression on flagellar motor performance. (A) Enhanced motility of cells overexpressing H-NS in plates supplemented with NaCl. H-NS expression was induced by salicylate at the indicated concentrations. (B) Enhanced motility of the FliG D288N D289N double mutant upon overexpression of H-NS. The plate was incubated at 32°C for 16 h (salicylate concentration, 2.5 μM). (C) Effects of H-NS expression on motility in tryptone plates with various agar concentrations. (D) Low levels of H-NS can support motility on 0.38% (swim) agar but not on 0.5% (swarm) agar. (E) Disulfide cross-linking between Cys residues in $FliG_M$ (position 121) and in the helix linking $FliG_M$ to $FliG_C$ (position 179) and effects of H-NS deletion or overexpression. Cross-linking was induced using copper-phenanthroline in cells disrupted using lysozyme/EDTA/osmotic lysis. Blots were probed with anti-HA antibody. $FliG_{NM}$, FliG N-terminal and middle domains; $FliG_C$, FliG C-terminal domain.

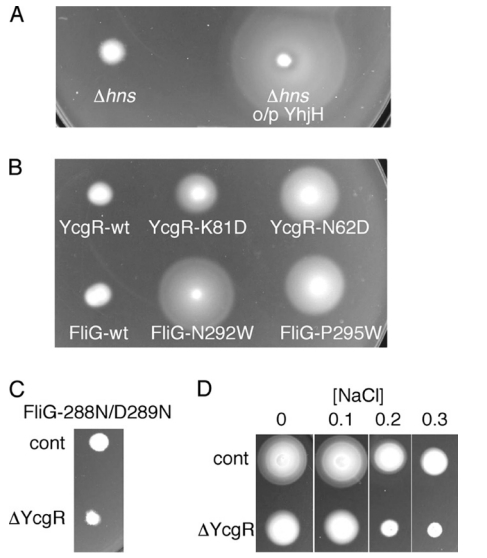

FIG. 5. (A) Enhanced motility of the Δ*hns flhDC*-constitutive strain overexpressing the c-di-GMP hydrolase YhjH (through expression of *yhjH* from plasmid pKP77 with induction by 2.5 μM salicylate). (B) Enhanced motility of the Δ*hns flhDC*-constitutive strain harboring mutations that weaken the YcgR-FliG interaction (45). (C) Effect of the YcgR deletion on motility of the D288N D289N mutant (contrast with Fig. 4B). (D) Effect of the YcgR deletion on motility at high ionic strength (contrast with Fig. 4A).

Both showed efficient intramolecular cross-linking on treatment with oxidizing agent (data are shown in Fig. 4E for positions 121 and 179; similar results were obtained for positions 121 and 183). Yield of the $FliG_{121}$/$FliG_{179}$ cross-link was substantially decreased upon overexpression of H-NS and was increased in the Δ*hns* strain (Fig. 4E).

Interplay between H-NS and YcgR. The cyclic-di-GMP binding protein YcgR has recently been shown to regulate flagellar motility by mechanisms that involve both FliG and FliM on the rotor (16, 45) and the MotA protein of the stator (10). When bound to cyclic-di-GMP, YcgR inhibits motility by altering both the speed and directional bias of motor rotation. As an inhibitor of motility, the effect of YcgR is, in a rough sense, opposite that of H-NS, and the first indication of a role for YcgR in motility came in the suppressor screen of Ko and Park (26), in which loss of *ycgR* was found to rescue the motility defect in a Δ*hns* strain. To examine the interplay between H-NS and YcgR further, we measured the motility of Δ*hns* cells containing point mutations that weaken the YcgR-FliG interaction (45). Mutations in both YcgR and FliG were tested and in both cases allowed substantially improved motility of the Δ*hns* strain (Fig. 5). Thus, a part of the motility defect in the Δ*hns* cell is related to the presence of YcgR bound to the rotor. We next tested whether cells lacking YcgR performed better under conditions of a weakened rotor-stator interface. Cells lacking YcgR migrated more slowly than wild-type cells in high-salt plates, in contrast to the H-NS-overexpressing cells that showed enhanced motility. The YcgR deletion also did not improve motility of cells harboring the FliG double mutation D288N D289N (Fig. 5). The contrasting effects of YcgR deletion and H-NS overexpression indicate that H-NS does not act solely in opposition to YcgR but exerts its own influence on the rotor-stator interface. A model that can account for the actions of H-NS and YcgR, in the framework of the working model for rotor structure (43), is discussed below.

DISCUSSION

The present results show that H-NS binds to the highly conserved EHPQR motif in $FliG_M$ as a dimer to organize the FliG subunits in the rotor and stabilize the rotor-stator interface. The H-NS homolog StpA binds to the same region of FliG and appears to act similarly. While H-NS has not been identified in purified basal body preparations, presumably because it does not bind strongly enough to survive purification steps, its effects on motility (Fig. 4) and on FliG cross-linking *in vivo* (Fig. 1) indicate that it interacts with the motors in cells and has a large influence on motor performance. Our working model of switch complex architecture allows the action of H-NS to be rationalized in structural terms. The $FliG_M$ domain that binds H-NS occupies a bridging position between the central (i.e., nearer the axis) parts of the rotor and the $FliG_C$ domains at the perimeter. The electron microscopy (EM) reconstructions show only a tenuous connection between the MS ring and the parts assigned to $FliG_N$ and $FliG_M$ domains (43, 58), and according to the switch complex model, most of the $FliG_M$ domains are not directly supported by $FliM_M$ (13, 43) (Fig. 6). Thus, $FliG_M$ and the helix linking it to $FliG_C$ have the character of a spoke, and the rigidity of these elements should be a key factor in the appropriate positioning and stabilization of $FliG_C$ at the rotor-stator interface. By binding to $FliG_M$, on a surface near the linking helix, H-NS could modulate the rigidity and/or orientation of the spokes.

Ko and Park (26) found that H-NS is less critical for flagellar motor function when the motility inhibitor YcgR is also absent from the cell. The present results show that motility in the Δ*hns* background is also improved by mutations that weaken the interaction of YcgR with FliG (Fig. 5B). Thus, the interplay between these motility regulators appears to occur within the motor, where each binds to FliG. While the effects of H-NS and YcgR are in a general sense opposite, with the one enhancing and the other impairing motor function, the present results also show that H-NS does not act only in opposition to YcgR but exerts its own, evidently stabilizing, influence upon the rotor-stator interface. A structural model that rationalizes the actions of H-NS and YcgR is shown in Fig. 6. As described previously (45), YcgR is proposed to bind to $FliM_M$ and $FliG_C$ in the outer part of the rotor, and upon binding c-di-GMP reorients $FliG_C$ to disrupt its interactions with the stator (45). YcgR also interacts with the stator protein MotA (10) and might also, besides disrupting the normal FliG-MotA interaction, introduce friction at the rotor-stator interface. On the basis of the present results, H-NS is proposed to interact with the FliG middle domain to alter the position or flexibility of the $FliG_M$-$FliG_C$-linking helix so that $FliG_C$ is held in a more stable relationship to the stator (Fig. 6B, left). Because H-NS stabilizes the normal conformation of $FliG_C$, it should act to oppose the YcgR-induced $FliG_C$ reorientation, thus accounting for the observation that Δ*hns* mutants are particularly susceptible to the action of YcgR.

It is presently not clear why H-NS, an abundant DNA-binding protein, is a suitable protein to regulate performance

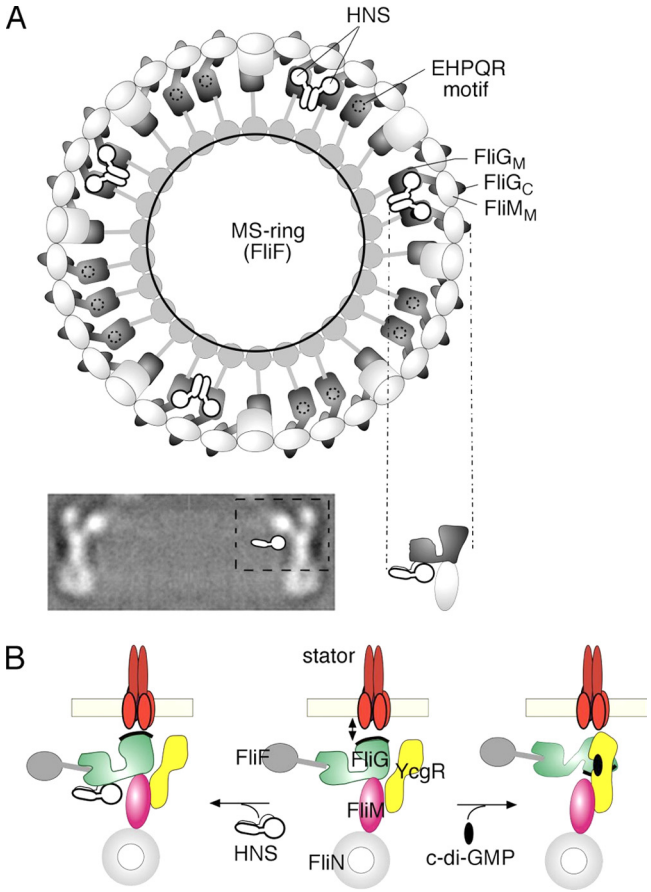

FIG. 6. Model for H-NS action at the flagellar motor. (A) Plan view of the switch complex (43). The hypothesized H-NS-binding site is indicated. Because most $FliM_M$ domains are in the outer position, the EHPQR motifs of most $FliG_M$ domains would be available to bind H-NS. Four H-NS dimers are shown bound to the rotor, but the actual number is likely to vary. A FliG/FliM/$FliN_4$ element is shown below in side view, with the EM reconstruction of the C ring shown for comparison. (B) Interplay of H-NS and YcgR in regulating the function of the switch complex. The middle state represents the switch complex in the absence of any strong influence from H-NS or YcgR. YcgR is hypothesized to bind to FliM in the absence of c-di-GMP but without strongly affecting motor function. c-di-GMP binding is proposed to induce rearrangements in the rotor illustrated in the right-hand state (similar to those described previously [45]). A working hypothesis for H-NS action is shown on the left. H-NS is proposed to alter the position or stability of the helix linking the $FliG_M$ and $FliG_C$ domains (the "spokes") to stabilize the rotor-stator interface.

of the flagellar motor. H-NS regulates transcription of a wide variety of genes but has been implicated particularly in the responses to temperature, pH, and osmolarity (2, 62, 63). Binding of H-NS to DNA is weakened at high ionic strength (1, 33), a property that might be important in osmosensing. The responses of H-NS to ionic strength and temperature, to the extent that they alter its affinity for DNA and its availability for binding FliG, might also figure in the present context; for example, as intracellular ionic strength increased, the dissociation of H-NS from the chromosome might increase its availability for binding to FliG. In this scenario, H-NS would function to dynamically tune the rotor-stator interface to changing circumstances of ionic strength, osmolarity, or temperature.

We note, in conclusion, that the present identification of an H-NS binding site on the EHPQR motif lends additional support to the present model for rotor organization. According to the model, most $FliM_M$ domains are positioned under $FliG_C$, leaving most $FliG_M$ domains available to bind H-NS (Fig. 6). In two recently proposed alternative models (31, 40), each $FliG_M$ domain is bound to $FliM_M$, and because this binding occurs via the EHPQR motif and surrounding regions of $FliG_M$ (13, 43), binding of H-NS would be prevented.

ACKNOWLEDGMENTS

We thank Chankyu Park and Sandy Parkinson for strains and plasmids, Sandy Parkinson, Kelly Hughes, and members of the Blair laboratory for discussions, and Duncan Brunstetter for technical assistance with soft-agar motility assays.

This work was supported by grants RO1-GM64664 and GM087260Z from the U.S. National Institutes of Health.

REFERENCES

1. **Amit, R., A. B. Oppenheim, and J. Stavans.** 2003. Increased bending rigidity of single DNA molecules by HNS, a temperature and osmolarity sensor. Biophys. J. **84:**2467–2473.
2. **Atlung, t., and H. Ingmer.** 1997. H-NS: a modulator of environmentally regulated gene expression. Mol. Microbiol. **24:**7–17.
3. **Berg, H. C.** 2003. The rotary motor of bacterial flagella. Annu. Rev. Biochem. **72:**19–54.
4. **Berry, R. M., and H. C. Berg.** 1999. Torque generated by the flagellar motor of *Escherichia coli* while driven backward. Biophys. J. **76:**580–587.
5. **Bertin, P., et al.** 1994. The H-NS protein is involved in the biogenesis of flagella in *Escherichia coli*. J. Bacteriol. **176:**5537–5540.
6. **Blair, D. F., and H. C. Berg.** 1990. The MotA protein of *E. coli* is a proton-conducting component of the flagellar motor. Cell **60:**439–449.
7. **Blair, D. F., and H. C. Berg.** 1988. Restoration of torque in defective flagellar motors. Science **242:**1678–1681.
8. **Bloch, V., et al.** 2003. The H-NS dimerization domain defines a new fold contributing to DNA recognition. Nat. Struct. Biol. **10:**212–218.
9. **Block, S. M., and H. C. Berg.** 1984. Successive incorporation of force-generating units in the bacterial rotary motor. Nature **309:**470–472.
10. **Boehm, A., et al.** 2010. Second messenger-mediated adjustment of bacterial swimming velocity. Cell **141:**107–116.
11. **Brown, P. N., C. P. Hill, and D. F. Blair.** 2002. Crystal structure of the middle and C-terminal domains of the flagellar rotor protein FliG. EMBO J. **21:** 3225–3234.
12. **Brown, P. N., M. A. A. Mathews, L. A. Joss, C. P. Hill, and D. F. Blair.** 2005. Crystal structure of the flagellar rotor protein FliN from *Thermotoga maritima*. J. Bacteriol. **187:**2890–2902.
13. **Brown, P. N., M. Terrazas, K. Paul, and D. F. Blair.** 2007. Mutational analysis of the flagellar rotor protein FliG: sites of interaction with FliM and implications for organization of the switch complex. J. Bacteriol. **189:**305–312.
14. **Chilcott, G. S., and K. T. Hughes.** 2000. Coupling of flagellar gene expression to flagellar assembly in *Salmonella enterica* serovar Typhimurium and *Escherichia coli*. Microbiol. Mol. Biol. Rev. **64:**694–708.
15. **Donato, G. M., and T. H. Kawula.** 1998. Enhanced binding of altered H-NS protein to flagellar rotor protein FliG causes increased flagellar rotational speed and hypermotility in *Escherichia coli*. J. Biol. Chem. **273:**24030–24036.
16. **Fang, X., and M. Gomelsky.** 2010. A post-translational, c-di-GMP-dependent mechanism regulating flagellar motility. Mol. Microbiol. **76:**1295–1305.
17. **Francis, N. R., V. M. Irikura, S. Yamaguchi, D. J. DeRosier, and R. M. Macnab.** 1992. Localization of the *Salmonella typhimurium* flagellar switch protein FliG to the cytoplasmic M-ring face of the basal body. Proc. Natl. Acad. Sci. U. S. A. **89:**6304–6308.
18. **Francis, N. R., G. E. Sosinsky, D. Thomas, and D. J. DeRosier.** 1994. Isolation, characterization and structure of bacterial flagellar motors containing the switch complex. J. Mol. Biol. **235:**1261–1270.
19. **Glagolev, A. N., and V. P. Skulachev.** 1978. The proton pump is a molecular engine of motile bacteria. Nature **272:**280–282.
20. **Harshey, R. M.** 1994. Bees aren't the only ones: swarming in Gram-negative bacteria. Mol. Microbiol. **13:**389–394.
21. **Hirota, N., M. Kitada, and Y. Imae.** 1981. Flagellar motors of alkalophilic *Bacillus* are powered by an electrochemical potential gradient of Na^+. FEBS Lett. **132:**278–280.
22. **Irikura, V. M., M. Kihara, S. Yamaguchi, H. Sockett, and R. M. Macnab.** 1993. *Salmonella typhimurium fliG* and *fliN* mutations causing defects in assembly, rotation, and switching of the flagellar motor. J. Bacteriol. **175:** 802–810.

23. **Johansson, J., S. Eriksson, B. Sonden, S. N. Wai, and B. E. Uhlin.** 2001. Heteromeric interactions among nucleoid-associated bacterial proteins: localization of Stp-A stabilizing regions in H-NS of *Escherichia coli*. J. Bacteriol. **183:**2343–2347.
24. **Johansson, J., and B. E. Uhlin.** 1999. Differential protease-mediated turnover of H-NS and StpA revealed by a mutation altering protein stability and stationary-phase survival of *Escherichia coli*. Proc. Natl. Acad. Sci. U. S. A. **96:**10776–10781.
25. **Khan, S., M. Dapice, and T. S. Reese.** 1988. Effects of *mot* gene expression on the structure of the flagellar motor. J. Mol. Biol. **202:**575–584.
26. **Ko, M., and C. Park.** 2000. Two novel flagellar components and H-NS are involved in the motor function of *Escherichia coli*. J. Mol. Biol. **303:**371–382.
27. **Kohno, T., and J. R. Roth.** 1979. Electrolyte effects on the activity of mutant enzymes in vivo and in vitro. Biochemistry **18:**1386–1392.
28. **Kojima, S., and D. F. Blair.** 2001. Conformational change in the stator of the bacterial flagellar motor. Biochemistry **40:**13041–13050.
29. **Kojima, S., and D. F. Blair.** 2004. Solubilization and purification of the MotA/MotB complex of *Escherichia coli*. Biochemistry **43:**26–34.
30. **Larsen, S. H., J. Adler, J. J. Gargus, and R. W. Hogg.** 1974. Chemomechanical coupling without ATP: the source of energy for motility and chemotaxis in bacteria. Proc. Natl. Acad. Sci. U. S. A. **71:**1239–1243.
31. **Lee, L. K., M. A. Ginsburg, C. Crovace, M. Donohoe, and D. Stock.** 2010. Structure of the torque ring of the flagellar motor and the molecular basis for rotational switching. Nature **466:**996–1000.
32. **Li, H., and V. Sourjik.** 2011. Assembly and stability of flagellar motor in *Escherichia coli*. Mol. Microbiol. **80:**886–899.
33. **Liu, Y., H. Chen, L. J. Kenney, and J. Yan.** 2010. A divalent switch drives H-NS/DNA-binding conformations between stiffening and bridging modes. Genes Dev. **24:**339–344.
34. **Lloyd, S. A., and D. F. Blair.** 1997. Charged residues of the rotor protein FliG essential for torque generation in the flagellar motor of *Escherichia coli*. J. Mol. Biol. **266:**733–744.
35. **Lloyd, S. A., H. Tang, X. Wang, S. Billings, and D. F. Blair.** 1996. Torque generation in the flagellar motor of *Escherichia coli*: evidence of a direct role for FliG but not for FliM or FliN. J. Bacteriol. **178:**223–231.
36. **Lowder, B. J., M. D. Duyvesteyn, and D. F. Blair.** 2005. FliG subunit arrangement in the flagellar rotor probed by targeted cross-linking. J. Bacteriol. **187:**5640–5647.
37. **Macnab, R. M.** 2003. How bacteria assemble flagella. Annu. Rev. Microbiol. **57:**77–100.
38. **Marykwas, D. L., S. A. Schmidt, and H. C. Berg.** 1996. Interacting components of the flagellar motor of *Escherichia coli* revealed by the two-hybrid system in yeast. J. Mol. Biol. **256:**564–576.
39. **Mathews, M. A. A., H. L. Tang, and D. F. Blair.** 1998. Domain analysis of the FliM protein of *Escherichia coli*. J. Bacteriol. **180:**5580–5590.
40. **Minamino, T., et al.** 2011. Structural insight into the rotational switching mechanism of the bacterial flagellar motor. PLoS Biol. **9:**e1000616.
41. **Park, S. Y., B. Lowder, A. M. Bilwes, D. F. Blair, and B. R. Crane.** 2006. Structure of FliM provides insight into assembly of the switch complex in the bacterial flagella motor. Proc. Natl. Acad. Sci. U. S. A. **103:**11886–11891.
42. **Paul, K., and D. F. Blair.** 2006. Organization of FliN subunits in the flagellar motor of *E. coli*. J. Bacteriol. **188:**2502–2511.
43. **Paul, K., G. Gonzalez-Benet, A. Bilwes, B. Crane, and D. Blair.** 2011. Architecture of the flagellar rotor. EMBO J. **30:**2962–2971.
44. **Paul, K., J. Harmon, and D. F. Blair.** 2006. Mutational analysis of the flagellar rotor protein FliN: identification of surfaces important for flagellar assembly and switching. J. Bacteriol. **188:**5240–5248.
45. **Paul, K., V. M. Nieto, W. Carlquist, D. F. Blair, and R. M. Harshey.** 2010. The c-di-GMP binding protein YcgR controls flagellar motor direction and speed to affect chemotaxis by a "backstop brake" mechanism. Mol. Cell **38:**128–139.
46. **Reid, S. W., et al.** 2006. The maximum number of torque-generating units in the flagellar motor of *Escherichia coli* is at least 11. Proc. Natl. Acad. Sci. U. S. A. **103:**8066–8071.
47. **Rimsky, S.** 2004. Structure of the histone-like protein H-NS and its role in regulation and genome superstructure. Curr. Opin. Microbiol. **7:**109–114.
48. **Sarkar, M. K., K. Paul, and D. Blair.** 2010. Chemotaxis signaling protein CheY binds to the rotor protein FliN to control the direction of flagellar rotation in *Escherichia coli*. Proc. Natl. Acad. Sci. U. S. A. **107:**9370–9375.
49. **Sarkar, M. K., K. Paul, and D. F. Blair.** 2010. Subunit organization and reversal-associated movements in the flagellar switch of *Escherichia coli*. J. Biol. Chem. **285:**675–684.
50. **Sato, K., and M. Homma.** 2000. Functional reconstitution of the Na^+-driven polar flagellar motor component of *Vibrio alginolyticus*. J. Biol. Chem. **275:**5718–5722.
51. **Shindo, H., et al.** 1995. Solution structure of the DNA binding domain of a nucleoid-associated protein, H-NS, from *Escherichia coli*. FEBS Lett. **360:**125–131.
52. **Sockett, H., S. Yamaguchi, M. Kihara, V. M. Irikura, and R. M. Macnab.** 1992. Molecular analysis of the flagellar switch protein FliM of *Salmonella typhimurium*. J. Bacteriol. **174:**793–806.
53. **Soutourina, O., et al.** 1999. Multiple control of flagellum biosynthesis in *Escherichia coli*: role of H-NS protein and the cyclic AMP-catabolite activator protein complex in transcription of the *flhDC* master operon. J. Bacteriol. **181:**7500–7508.
54. **Suzuki, H., K. Yonekura, and K. Namba.** 2004. Structure of the rotor of the bacterial flagellar motor revealed by electron cryo-microscopy and single-particle image analysis. J. Mol. Biol. **337:**105–113.
55. **Tang, H., S. Billings, X. Wang, L. Sharp, and D. F. Blair.** 1995. Regulated underexpression and overexpression of the FliN protein of *Escherichia coli* and evidence for an interaction between FliN and FliM in the flagellar motor. J. Bacteriol. **177:**3496–3503.
56. **Tang, H., and D. F. Blair.** 1995. Regulated underexpression of the FliM protein of *Escherichia coli* and evidence for a location in the flagellar motor distinct from the MotA/MotB torque generators. J. Bacteriol. **177:**3485–3495.
57. **Tang, H., T. F. Braun, and D. F. Blair.** 1996. Motility protein complexes in the bacterial flagellar motor. J. Mol. Biol. **261:**209–221.
58. **Thomas, D. R., N. R. Francis, C. Xu, and D. J. DeRosier.** 2006. The three-dimensional structure of the flagellar rotor from a clockwise-locked mutant of *Salmonella enterica* serovar Typhimurium. J. Bacteriol. **188:**7039–7048.
59. **Thomas, D. R., D. G. Morgan, and D. J. DeRosier.** 1999. Rotational symmetry of the C ring and a mechanism for the flagellar rotary motor. Proc. Natl. Acad. Sci. U. S. A. **96:**10134–10139.
60. **Ueguchi, C., T. Suzuki, T. Yoshida, K. Tanaka, and T. Mizuno.** 1996. Systematic mutational analysis revealing the functional domain organization of *Escherichia coli* nucleoid protein H-NS. J. Mol. Biol. **263:**149–162.
61. **Welch, M., K. Oosawa, S.-I. Aizawa, and M. Eisenbach.** 1993. Phosphorylation-dependent binding of a signal molecule to the flagellar switch of bacteria. Proc. Natl. Acad. Sci. U. S. A. **90:**8787–8791.
62. **White-Ziegler, C., and T. R. Davis.** 2009. Genome-wide identification of H-NS-controlled, temperature-regulated genes in *Escherichia coli* K-12. J. Bacteriol. **191:**1106–1110.
63. **Williams, R. M., and S. Rimsky.** 1997. Molecular aspects of the *Escherichia coli* nucleoid protein, H-HS: a central controller of gene regulatory networks. FEMS Microbiol. Lett. **156:**175–185.
64. **Yakushi, T., J. Yang, H. Fukuoka, M. Homma, and D. F. Blair.** 2006. Roles of charged residues of rotor and stator in flagellar rotation: comparative study using H^+-driven and Na^+-driven motors in *Escherichia coli*. J. Bacteriol. **188:**1466–1472.
65. **Yamaguchi, S., et al.** 1986. Genetic evidence for a switching and energy-transducing complex in the flagellar motor of *Salmonella typhimurium*. J. Bacteriol. **168:**1172–1179.
66. **Young, H. S., H. Dang, Y. Lai, D. J. DeRosier, and S. Khan.** 2003. Variable symmetry in *Salmonella typhimurium* flagellar motors. Biophys. J. **84:**571–577.
67. **Zhao, R., C. D. Amsler, P. Matsumura, and S. Khan.** 1996. FliG and FliM distribution in the *Salmonella typhimurium* cell and flagellar basal bodies. J. Bacteriol. **178:**258–265.
68. **Zhou, J., and D. F. Blair.** 1997. Residues of the cytoplasmic domain of MotA essential for torque generation in the bacterial flagellar motor. J. Mol. Biol. **273:**428–439.
69. **Zhou, J., S. A. Lloyd, and D. F. Blair.** 1998. Electrostatic interactions between rotor and stator in the bacterial flagellar motor. Proc. Natl. Acad. Sci. U. S. A. **95:**6436–6441.
70. **Zhou, J., et al.** 1998. Function of protonatable residues in the flagellar motor of *Escherichia coli*: a critical role for Asp 32 of MotB. J. Bacteriol. **180:**2729–2735.